Electrochemistry

DOI: 10.1002/anie.201003485

Fabrication of Graphene-Encapsulated Oxide Nanoparticles: Towards High-Performance Anode Materials for Lithium Storage**

Shubin Yang, Xinliang Feng, Sorin Ivanovici, and Klaus Müllen**

Electrochemically active metals and metal oxides such as Sn,[1] Si,[2] SnO_2,[3] and Co_3O_4[4] have long been considered as anode materials for lithium ion batteries because of their high theoretical capacities. However, a large specific volume change commonly occurs in the host matrix of these metals and metal oxides during the cycling processes, thus leading to pulverization of the electrodes and rapid capacity decay.[1–3] To circumvent these obstacles, carbonaceous materials with high electrical conductivity and fair ductility have been widely chosen as matrices for metals and metal oxides to improve their cycle performance. In particular, graphene, which is a monolayer of carbon atoms arranged in a honeycomb network, is becoming one of the most appealing matrices because of its unique properties such as superior electrical conductivity,[5] excellent mechanical flexibility,[6] large surface area ($2630\ m^2\,g^{-1}$),[7] and high thermal and chemical stability.[8] In this regard, Si/graphene,[9] SnO_2/graphene,[10] TiO_2/graphene,[11] and Co_3O_4/graphene[12] hybrids or composites, in which metals or metal oxides are distributed onto the surface of graphene or between the graphene layers, have been fabricated by restacking graphene sheets in the presence of guest nanoparticles or corresponding organometallic precursors. Compared to other carbon matrices such as graphite,[13] carbon black,[14] and carbon nanotubes,[15] graphene sheets can more effectively buffer the strain from the volume change of metals or metal oxides during the charging–discharging processes and preserve the high electrical conductivity of the overall electrode. Nevertheless, the metal and metal oxide nanoparticles are still prone to strong aggregation during the cycle processes because of nonintimate contact between graphene layers and active nanoparticles.[7–10] This leads to a decrease in capacity of most metal or metal oxide/graphene composites by 20–50% of their first reversible capacity after 30 cycles.[9–10] One of the most promising strategies to tackle the aggregation problem of metal and metal oxides in lithium ion batteries is to confine them within individual carbon shells.[16–19] A key challenge in this strategy is the achievement of both high electrical conductivity and a low-weight fraction of thin carbon layers on the surface of metal or metal oxide nanoparticles.

Herein we describe a novel strategy for the fabrication of graphene-encapsulated metal oxide (GE–MO) by coassembly between negatively charged graphene oxide and positively charged oxide nanoparticles. The process is driven by the mutual electrostatic interactions of the two species, and is followed by chemical reduction. The resulting GE–MO possesses flexible and ultrathin graphene shells that effectively enwrap the oxide nanoparticles. This unique hybrid architecture can 1) suppress the aggregation of oxide nanoparticles, 2) accommodate the volume change during the cycle processes, 3) give rise to a high oxide content in the composite (up to 91.5% by weight), and 4) maintain a high electrical conductivity of the overall electrode. As a consequence, graphene-encapsulated electrochemically active Co_3O_4 nanoparticles (GE–Co_3O_4) exhibit a very high reversible capacity of $1100\ mA\,h\,g^{-1}$ in the first 10 cycles, and over $1000\ mA\,h\,g^{-1}$ after 130 cycles, with excellent cycle performance, thus holding great potential as an anode material for lithium storage.

The overall synthetic procedure of GE–MO involves three steps (Figure 1): oxide nanoparticles were firstly modified by surface grafting of aminopropyltrimethoxysilane

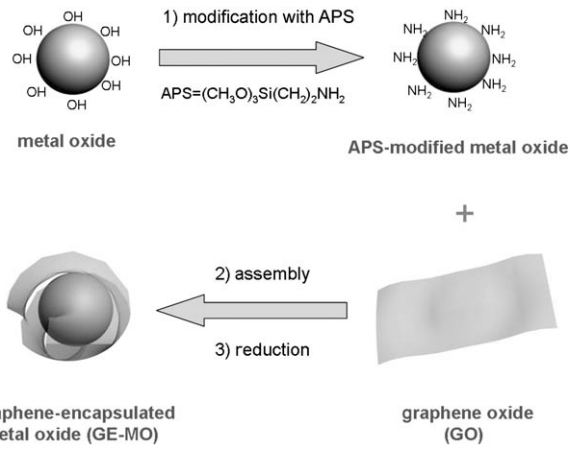

Figure 1. Fabrication of graphene-encapsulated metal oxide (GE–MO) including 1) modification of the metal oxide by grafting aminopropyltrimethoxysilane (APS) to render the oxide surface positively charged; 2) hybrid assembly between positively charged oxide nanoparticles and negatively charged graphene oxide by electrostatic interactions; and 3) chemical reduction.

[*] Dr. S. Yang, Dr. X. Feng, Prof. Dr. K. Müllen
Max-Planck-Institut für Polymerforschung
Ackermannweg 10, 55128 Mainz (Germany)
Fax: (+49) 6131-379-350
E-mail: feng@mpip-mainz.mpg.de
muellen@mpip-mainz.mpg.de
Dr. S. Ivanovici
BASF SE, GVC/F-J550
67056 Ludwigshafen (Germany)

[**] This work was financially supported by the Max Planck Society through the program ENERCHEM, the German Science Foundation (Korean–German IRTG), and the DFG Priority Program SPP 1355. We also thank Prof. Dr. Joachim Maier and Dr. Kun Tang for helpful discussions.

Supporting information for this article is available on the WWW under http://dx.doi.org/10.1002/anie.201003485.

(APS)[20] to render the oxide surface positively charged (Figure 2a and Figure S1 in Supporting Information). The modified oxide nanoparticles were then assembled with negatively charged graphene oxide by electrostatic interactions. Under optimal conditions, almost all the graphene oxide and modified oxide nanoparticles coassembled to leave a transparent aqueous solution (Figure S2 in the Supporting Information). Finally, the resulting aggregates were chemically reduced with hydrazine to result in graphene-encapsulated oxide nanoparticles.

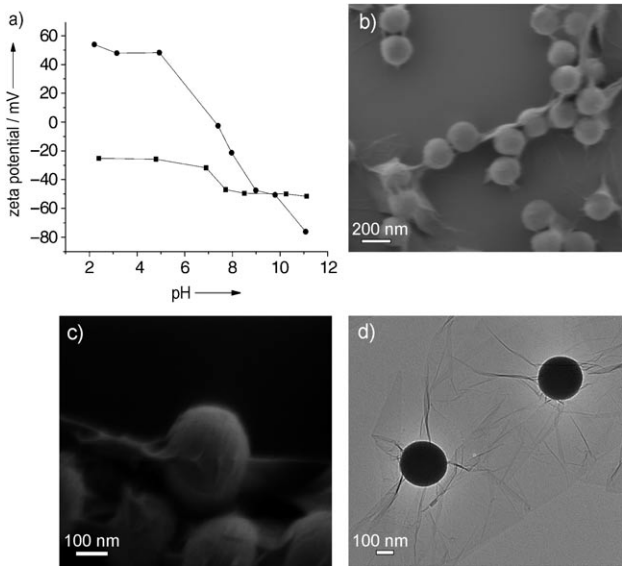

Figure 2. a) Zeta potentials of APS-modified silica (●) and graphene oxide (■) in aqueous solutions with various pH values; b, c) typical SEM, and d) TEM images of graphene-encapsulated silica spheres.

We initially tested our concept by producing graphene-encapsulated silica spheres (GE–silica) in aqueous solutions with different pH values. In the pH range 2.0–8.0, the precipitates spontaneously formed as soon as the modified silica was diluted into the graphene oxide suspension (Figure S2 in the Supporting Information). In contrast, at pH values above 8.0, both the modified silica and graphene oxide were stably dispersed in the solution and thus no assembly occurred between the two components. To direct the assembly by adopting the appropriate pH values, the surface charges of modified silica spheres and graphene oxide were further examined by zeta potential measurements. As shown in Figure 2a, the surface of graphene oxide was negatively charged (zeta potential = −25–52 mV) over the investigated pH range (2–11). Apparently, this charge originated from the ionization of the carboxylic acid and phenolic hydroxy groups that were located on the graphene oxide.[21] The surface charge of the modified silica switched from positive (zeta potential = +54 mV) to negative (zeta potential = −76 mV) with an increase of the pH value from 2 to 11. It follows that the mutual assembly can only be triggered when modified silica and graphene oxide were oppositely charged, thus suggesting that the electrostatic interaction was the driving force.

The morphology and structure of the resulting GE–silica were elucidated by SEM, TEM, and high-resolution TEM (HRTEM) measurements (Figure 2b, c). The graphene-encapsulated spheres showed crinkled and rough textures that were associated with the presence of flexible and ultrathin graphene sheets. In most cases, the edges of individual as well as overlapping graphene layers could be observed, particularly at the interface between aggregated particles, where the graphene layers appeared to link neighboring spheres together (Figure 2b). Cross-sectional TEM and HRTEM images (Figure 2d and Figure S3 in Supporting Information) confirmed the extremely thin (< 3 nm), flexible, and corrugated nature of the graphene shells. Remarkably, after removal of the silica spheres by etching with a 2 M NaOH solution, hollow graphene spheres with thin and intact continuous walls were formed (Figure S3b in the Supporting Information). This result suggests an intimate encapsulation of the silica spheres by graphene sheets, and is consistent with the SEM observations (Figure 1b, c).

Such a coassembly protocol can be further extended to the construction of core–shell hybrid architectures consisting of electrochemically active metal oxides and ultrathin, flexible graphene shells. Typically, the graphene-encapsulated Co_3O_4 composite (GE–Co_3O_4) was successfully fabricated by using APS-modified Co_3O_4 nanoparticles instead of modified silica, owing to their similar positively charged surfaces (Figure 3a–c, Figures S4 and S5 in the Supporting Information). The typical SEM images (Figure 3b, c) of GE–Co_3O_4 revealed that the graphene sheets were wrapped around the surface of Co_3O_4 nanoparticles. The resultant GE–Co_3O_4 composites

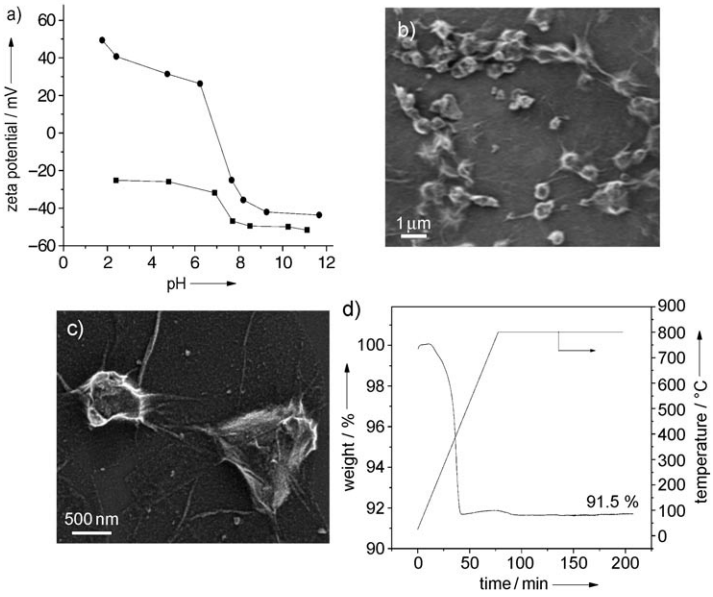

Figure 3. a) Zeta potentials of APS-modified Co_3O_4 (●) and graphene oxide (■) in aqueous solution at different pH values; b, c) typical SEM images, and d) TGA curve of graphene-encapsulated Co_3O_4.

were further characterized by X-ray diffraction. Remarkably, all the diffraction peaks of the GE–Co_3O_4 were perfectly indexed to the cubic spinel Co_3O_4 with a lattice parameter of $a = 8.01$ Å.[12,22] Moreover, no conventional stacking peak of graphene sheets at $2\theta = 26.6°$ was detected (Figure S6 in the Supporting Information), thus suggesting that the graphene sheets were homogeneously dispersed onto the surface of Co_3O_4 nanoparticles. Thermogravimetric analysis (TGA) of GE–Co_3O_4 (Figure 3d) revealed that the weight fraction of Co_3O_4 in the composite is as high as 91.5%, which is much higher than those of reported core–shell metal and metal oxide/carbon composites (40–75%).[3,16,17b,18] Such a high content of Co_3O_4 in the composite, in association with flexible, ultrathin graphene shells as the buffer matrix and conducting pathways, must result in high capacity and excellent cycle performance when they are applied to lithium storage (see below).

Cyclic voltammetry (CV) experiments were conducted to evaluate the electrochemical performance of GE–Co_3O_4 at a scanning rate of 0.1 mV s^{-1} over the voltage range 0.01–3.00 V (Figure S7 in the Supporting Information). For comparison, bare Co_3O_4 nanoparticles were also tested under the same electrochemical conditions. In the case of GE–Co_3O_4, two reduction and three oxidation peaks were clearly observed in the first scanning curve. The first dominant reduction peak was at around 0.8 V, which can be attributed to the reduction reaction of Co_3O_4 with Li and the formation of solid electrolyte interphase (SEI) films on the surface of GE-Co_3O_4,[23] since it also appears in the CV of bare Co_3O_4. The second small reduction peak at 0.1 V and the first two oxidation peaks at 1.1 and 1.6 V were attributed to the insertion of lithium into reduced graphene sheets.[24] The third dominant oxidation peak at 2.1 V is characteristic of the reformation of Co_3O_4 from Co and Li_2O,[4,25] and is similar to that of bare Co_3O_4. The CV behavior of GE–Co_3O_4 confirms that both the graphene layers and Co_3O_4 are electrochemically active components for lithium storage. The overall capacity of GE–Co_3O_4 arises mainly from the properties of the metal oxide, thus further confirming the low content of graphene materials in the composite.

The capacity and cycle performance of GE–Co_3O_4 and bare Co_3O_4 electrodes were evaluated by galvanostatic discharge–charge measurements at a current density of 74 mA g^{-1} (Figure 4). It is striking to note that a very high and stable reversible capacity of about 1100 mA h g^{-1} in the initial 10 cycles, and 1000 mA h g^{-1} after 130 cycles were achieved for the GE-Co_3O_4 electrode (Figure 4). To the best of our knowledge, these values are the highest among all Co_3O_4 electrodes reported to date (600–850 mA h g^{-1}) at 74 mA g^{-1}.[22,25] Such a superior reversible capacity and excellent cycle performance can certainly be attributed to the synergistic effect between the flexible, thin graphene shells and the Co_3O_4 nanoparticles, despite the fact that the content of graphene in GE–Co_3O_4 is less than 10%. For comparison, we fabricated a Co_3O_4/graphene composite with the same Co_3O_4/graphene ratio (91.5:8.5) by simple mechanical blending. The mixed Co_3O_4/graphene composite showed

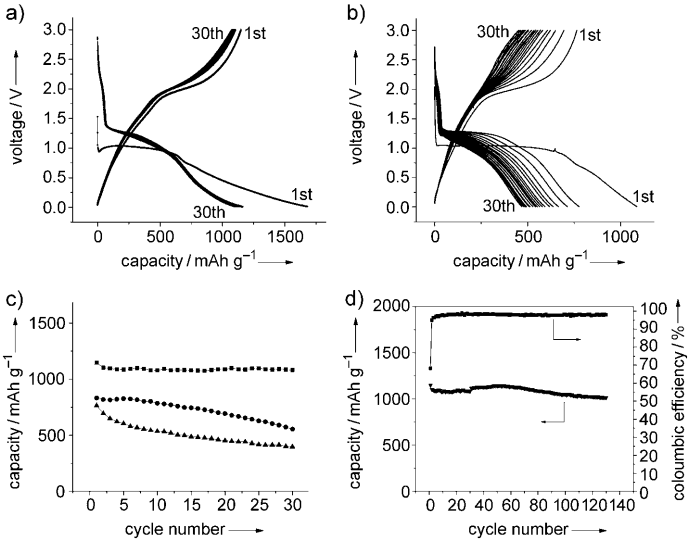

Figure 4. Galvanostatic discharge–charge profiles of a) GE–Co_3O_4 and b) bare Co_3O_4 electrodes (current density = 74 mA g^{-1}). Comparison of c) cycle performance of GE–Co_3O_4 (■), mixed Co_3O_4/graphene composite (●), and bare Co_3O_4 electrodes (▲) over 30 cycles, and d) cycle performance and Coulombic efficiency of the GE–Co_3O_4 electrode during 130 cycles (current density = 74 mA g^{-1}).

only a 67% retention of the initial capacity (832 mA h g^{-1}) after 30 cycles. Although this value is higher than that of bare Co_3O_4 (52%),[22] it is much lower than that of GE-Co_3O_4 (94%) after the same cycles. This result highlights again the value of our protocol.

In order to understand why GE–Co_3O_4 electrodes exhibit such a superior electrochemical performance compared to bare Co_3O_4 electrodes, AC impedance measurements were performed after 30 cycles. Nyquist plots (Figure 5) showed that the diameter of the semicircle for GE–Co_3O_4 electrodes in the high–medium frequency region was much smaller than that of bare Co_3O_4 electrodes, thus suggesting that GE–Co_3O_4 electrodes possess lower contact and charge-transfer impedances. The kinetic differences of GE–Co_3O_4 and bare Co_3O_4 electrodes were further investigated by modeling AC impendence spectra based on the modified Randles equivalent

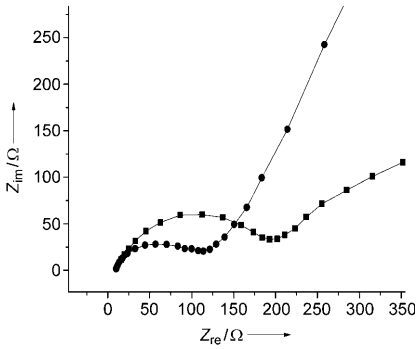

Figure 5. Nyquist plots of GE-Co_3O_4 (●) and bare Co_3O_4 (■) electrodes obtained by applying a sine wave with amplitude of 5.0 mV over the frequency range 100 kHz–0.01 Hz.

circuit[26] (Figure S8 in the Supporting information). The values of the film resistance R_f and charge-transfer resistance R_{ct} were 10.5 and 27.9 Ω respectively, in the case of GE-Co_3O_4, which were significantly lower than those of bare Co_3O_4 (27.8 and 97.9 Ω; Table S1 in the Supporting Information). This result confirmed that the graphene shells not only could preserve the high conductivity of the overall electrode, but also largely improve the electrochemical activity of metal oxides during the cycle processes.

In summary, we have demonstrated that graphene and metal oxides coassemble by electrostatic forces into core–shell hybrids. This assembly enables a good encapsulation of electrochemically active metal oxide nanoparticles by graphene sheets, thus leading to remarkable lithium-storage performance, including highly reversible capacity and excellent cycle performance. We believe that such a simple and low-cost assembly protocol will provide a new pathway for the large-scale production of various functional hybrid materials for energy storage.

Received: June 8, 2010
Published online: September 10, 2010

Keywords: cobalt oxides · electrochemistry · graphene · nanoparticles · silica

[1] D. Deng, J. Y. Lee, *Angew. Chem.* **2009**, *121*, 1688; *Angew. Chem. Int. Ed.* **2009**, *48*, 1660.
[2] C. K. Chan, H. L. Peng, G. Liu, K. McIlwrath, X. F. Zhang, R. A. Huggins, Y. Cui, *Nat. Nanotechnol.* **2008**, *3*, 31.
[3] W. M. Zhang, J. S. Hu, Y. G. Guo, S. F. Zheng, L. S. Zhong, W. G. Song, L. J. Wan, *Adv. Mater.* **2008**, *20*, 1160.
[4] P. Poizot, S. Laruelle, S. Grugeon, L. Dupont, J. M. Tarascon, *Nature* **2000**, *407*, 496.
[5] K. S. Novoselov, A. K. Geim, S. V. Morozov, D. Jiang, M. I. Katsnelson, I. V. Grigorieva, S. V. Dubonos, A. A. Firsov, *Nature* **2005**, *438*, 197.
[6] A. Fasolino, J. H. Los, M. I. Katsnelson, *Nat. Mater.* **2007**, *6*, 858.
[7] a) M. D. Stoller, S. J. Park, Y. W. Zhu, J. H. An, R. S. Ruoff, *Nano Lett.* **2008**, *8*, 3498; b) S. B. Yang, X. L. Feng, L. Wang, K. Tang, J. Maier, K. Müllen, *Angew. Chem.* **2010**, *122*, 4905; *Angew. Chem. Int. Ed.* **2010**, *49*, 4795.
[8] A. A. Balandin, S. Ghosh, W. Z. Bao, I. Calizo, D. Teweldebrhan, F. Miao, C. N. Lau, *Nano Lett.* **2008**, *8*, 902.
[9] J. K. Lee, K. B. Smith, C. M. Hayner, H. H. Kung, *Chem. Commun.* **2010**, *46*, 2025.
[10] a) S. M. Paek, E. Yoo, I. Honma, *Nano Lett.* **2009**, *9*, 72; b) J. Yao, X. P. Shen, B. Wang, H. K. Liu, G. X. Wang, *Electrochem. Commun.* **2009**, *11*, 1849.
[11] D. H. Wang, D. W. Choi, J. Li, Z. G. Yang, Z. M. Nie, R. Kou, D. H. Hu, C. M. Wang, L. V. Saraf, J. G. Zhang, I. A. Aksay, J. Liu, *Acs Nano* **2009**, *3*, 907.
[12] S. B. Yang, G. L. Cui, S. P. Pang, Q. Cao, U. Kolb, X. L. Feng, J. Maier, K. Müllen, *ChemSusChem* **2010**, *3*, 236.
[13] a) G. X. Wang, J. H. Ahn, M. J. Lindsay, L. Sun, D. H. Bradhurst, S. X. Dou, H. K. Liu, *J. Power Sources* **2001**, *211*, 97–98; b) N. Dimov, S. Kugino, A. Yoshio, *J. Power Sources* **2004**, *136*, 108.
[14] J. Park, J. Eom, H. Kwon, *Electrochem. Commun.* **2009**, *11*, 596.
[15] Z. P. Guo, Z. W. Zhao, H. K. Liu, S. X. Dou, *Carbon* **2005**, *43*, 1392.
[16] Y. S. Hu, R. Demir-Cakan, M. M. Titirici, J. O. Müller, R. Schlögl, M. Antonietti, J. Maier, *Angew. Chem.* **2008**, *120*, 1669; *Angew. Chem. Int. Ed.* **2008**, *47*, 1645.
[17] a) K. T. Lee, Y. S. Jung, S. M. Oh, *J. Am. Chem. Soc.* **2003**, *125*, 5652; b) G. L. Cui, Y. S. Hu, L. J. Zhi, D. Q. Wu, I. Lieberwirth, J. Maier, K. Müllen, *Small* **2007**, *3*, 2066.
[18] X. W. Lou, C. M. Li, L. A. Archer, *Adv. Mater.* **2009**, *21*, 2536.
[19] W. M. Zhang, X. L. Wu, J. S. Hu, Y. G. Guo, L. J. Wan, *Adv. Funct. Mater.* **2008**, *18*, 3941.
[20] a) B. Lee, Z. Ma, Z. T. Zhang, C. Park, S. Dai, *Microporous Mesoporous Mater.* **2009**, *122*, 160; b) J. S. Bridel, T. Azais, M. Morcrette, J. M. Tarascon, D. Larcher, *Chem. Mater.* **2010**, *22*, 1229.
[21] D. Li, M. B. Muller, S. Gilje, R. B. Kaner, G. G. Wallace, *Nat. Nanotechnol.* **2008**, *3*, 101.
[22] W. Y. Li, L. N. Xu, J. Chen, *Adv. Funct. Mater.* **2005**, *15*, 851.
[23] H. C. Liu, S. K. Yen, *J. Power Sources* **2007**, *166*, 478.
[24] G. X. Wang, X. P. Shen, J. Yao, J. Park, *Carbon* **2009**, *47*, 2049.
[25] a) Y. M. Kang, M. S. Song, J. H. Kim, H. S. Kim, M. S. Park, J. Y. Lee, H. K. Liu, S. X. Dou, *Electrochim. Acta* **2005**, *50*, 3667; b) M. H. Liang, L. J. Zhi, *J. Mater. Chem.* **2009**, *19*, 5871.
[26] a) S. B. Yang, X. L. Feng, L. J. Zhi, Q. A. Cao, J. Maier, K. Müllen, *Adv. Mater.* **2010**, *22*, 838; b) S. B. Yang, H. H. Song, X. H. Chen, *Electrochem. Commun.* **2006**, *8*, 137.

